Chemical Papers (2018) 72:2979–2985
https://doi.org/10.1007/s11696-018-0548-x

ORIGINAL PAPER

Synthesis of glycolysis inhibitor (*E*)-3-(pyridin-3-yl)-1-(pyridin-4-yl)prop-2-en-1-one (3PO) and its inhibition of HUVEC proliferation alone or in a combination with the multi-kinase inhibitor sunitinib

Miroslav Murár[1] · Jana Horvathová[2] · Roman Moravčík[2] · Gabriela Addová[3] · Michal Zeman[2] · Andrej Boháč[1,4]

Received: 26 May 2018 / Accepted: 28 June 2018 / Published online: 6 July 2018

Abstract

While a treatment of tumours by anti-angiogenic kinase inhibitors has limited efficacy and is associated with resistance and side effects, also other key biological pathways should be targeted to fight cancer more effectively. Active endothelial and cancer cells acquire energy predominantly via a glycolysis (Warburg effect) in contrast to most of other somatic cells preferring an oxidative phosphorylation. Proliferation of endothelial and cancer cells may be suppressed by a glycolysis inhibitor (*E*)-3-(pyridin-3-yl)-1-(pyridin-4-yl)prop-2-en-1-one (**3PO**) that synthesis is not sufficiently described in the literature. Moreover, a synergistic effect of inhibitors with different mechanisms of action may provide further advantages in cancer treatment. A combined effect of **3PO** with inhibitor of angiogenesis **sunitinib l-malate (SU)** was not yet investigated on HUVEC cells. We have developed a novel and efficient method for a synthesis of a glycolysis inhibitor **3PO**. The activity of **3PO** on HUVECs proliferation was investigated and its $IC_{50} = 10.7$ μM determined. By combination of **3PO** (10 μM) with **sunitinib l-malate** (0.1 μM) a significant synergistic effect on HUVECs proliferation was observed. Based on the structure, chemical reactivity and biological results, we proposed that **3PO** could be a multi-target inhibitor.

Keywords Synthesis · 3PO · Sunitinib · Inhibitor · PFKFB3 · Glycolysis · Kinases · HUVEC

Introduction

Deregulated angiogenesis is involved in a pathomechanism of several diseases, including cancer as the most significant of them. Inhibition of angiogenesis has recently become an attractive therapeutic possibility of cancer treatment (Kerbel and Folkman 2002). Angiogenesis is controlled by a complex of pro-angiogenic factors, among which vascular endothelial growth factor (VEGF) plays a key role. VEGF exhibits biological effects via binding to its plasma membrane receptors, preferentially type 2 (VEGFR2) (Carmeliet and Jain 2011). Therefore, efficient anti-angiogenic treatments are aimed either on neutralization of VEGF by its recombinant humanized monoclonal antibody **bevacizumab** (Ferrara et al. 2004) or interfering with post-receptor signal cascades. The second possibility comprises inhibition of biological effects of VEGF by blocking tyrosine kinase activity of its receptors. Multi-kinase inhibitors, e.g. (type I) inhibitor **sunitinib l-malate** (FDA, Pfizer 2006), exhibit more efficient action in comparison with more selectively

Electronic supplementary material The online version of this article (https://doi.org/10.1007/s11696-018-0548-x) contains supplementary material, which is available to authorized users.

The authors Jana Horvathová and Andrej Boháč contributed equally to writing this paper.

✉ Andrej Boháč
andrej.bohac@fns.uniba.sk

[1] Department of Organic Chemistry, Faculty of Natural Sciences, Comenius University in Bratislava, Mlynská dolina, Ilkovičova 6, 842 15 Bratislava, Slovakia

[2] Department of Animal Physiology and Ethology, Faculty of Natural Sciences, Comenius University in Bratislava, Mlynská dolina, Ilkovičova 6, 842 15 Bratislava, Slovakia

[3] Institute of Chemistry, Faculty of Natural Sciences, Comenius University in Bratislava, Mlynská dolina, Ilkovičova 6, 842 15 Bratislava, Slovakia

[4] Biomagi, Ltd., Mamateyova 26, 851 04 Bratislava, Slovakia

acting compounds. However, the higher efficiency can be accompanied with more serious side effects (Shaheen et al. 2001; Pla et al. 2014).

Both therapeutic strategies (anti-VEGF and anti-VEGFR2 TK) brought some successful results in cancer treatment but the development of resistance and side effects, especially on cardiovascular and nervous system (Tejpar et al. 2012), stimulates an extensive research on alternative treatment strategies (Pisarsky et al. 2016). In this context, inhibition of endothelial cell metabolism is one of the promising therapeutic possibilities (De Bock et al. 2013; Schoors et al. 2014). The strategy is based on the finding that both proliferating endothelial and tumour cells utilize glycolysis as a major source of energy for proliferation and migration (De Bock et al. 2013). Moreover, healthy mature endothelial cells, which form an inner side of blood vessels and utilize the oxidative phosphorylation for energy production, are in a quiescent state, but retain the ability to promptly proliferate in response to angiogenic signals (Zecchin et al. 2017). In this way, inhibition of glycolysis can provide several advantages since oxidative phosphorylation, as the major source of energy used by normal healthy human cells, can be only marginally affected. (*E*)-3-(pyridin-3-yl)-1-(pyridin-4-yl)prop-2-en-1-one (**3PO**) is known inhibitor of **PFKFB3** (6-phosphofructo-2-kinase/fructose-2,6-bisphosphatase) that reduces glycolytic flux and suppresses glucose uptake. **3PO** is selectively cytostatic to transformed cells and suppresses the growth of established tumour in mice (Conradi et al. 2017).

The aim of our study was to explore inhibitory effect of the glycolysis inhibitor **3PO** on proliferation of cultured human endothelial cells under in vitro conditions and to explore a potential synergistic effect of **3PO** together with a compound blocking the pathways activated by VEGF. Therefore, we studied the inhibition effect of HUVEC proliferation in response to **3PO** alone and in its combination with multi-kinase inhibitor (**sunitinib l-malate**) (Fig. 1).

Exploitation of **3PO** for in vivo studies on animals requires availability of its gram amounts. Access to **3PO** is rather limited. To prepare **3PO,** we searched its synthesis in the scientific databases (Reaxys 2018) and (SciFinder 2018). Instead of **3PO** only two complex side products **A** and **B** are formed by a reaction between nicotinaldehyde **1** and pyridinylethanone **2** catalysed by Na_2CO_3 at RT (Vatsadze et al. 2004) (Scheme 1).

In the older literature, the synthesis of **3PO** was described as the Claisen–Schmidt condensation between **1** and **2** catalysed by Et_2NH at RT (Durinda et al. 1966, 1967) or by KOH at 0 °C in MeOH/H_2O (5:1) (Jeong et al. 2011). We unsuccessfully tried to prepare **3PO** by different basic conditions (KOH, K_2CO_3, Et_3N, Et_2NH) at RT (or by cooling) within shorter or longer reaction time. By all of these reactions only traces of **3PO** were yielded in our hands with exception of the synthesis performed with Et_2NH by which 12% of **3PO** was obtained after chromatography (see Supplementary material). Based on the literature data and our experiences, we concluded that the synthesis and all currently required properties of **3PO** are not sufficiently known. Only M.p. of **3PO** (Durinda et al. 1966, 1967) and its ^{13}C-NMR spectrum (Liptaj et al. 1981 and WSS Inc. US 2018) can be found in the literature. Therefore, the development of a novel synthesis of **3PO** was required to ensure its broader availability.

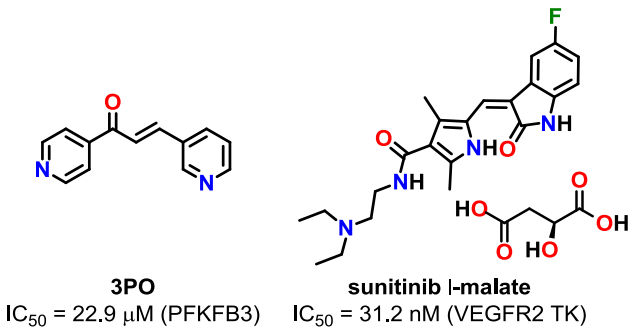

Fig. 1 The structures and activities of glycolysis inhibitor **3PO** (Clem et al. 2013 for IC_{50} = 22.9 μM) and VEGFR2 TKI **sunitinib l-malate** (Lintnerová et al. 2014 for IC_{50} = 31.2 nM)

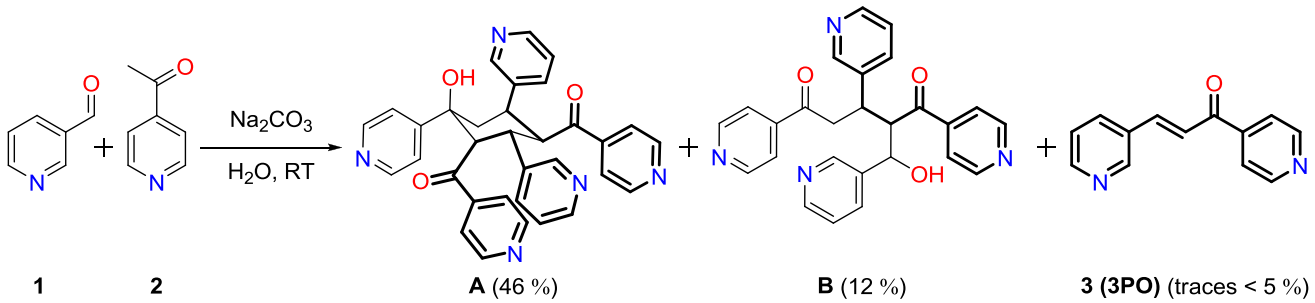

Scheme 1 The structures of products obtained after condensation of aldehyde **1** and ketone **2** performed under basic conditions at RT. Initially formed **3PO** was too sensitive on further transformations and mostly complex side products **A** and **B** were yielded. The structure of **3PO** and fragment(s) of **3PO** in the structures of the complex molecules **A** and **B** are marked in bold

Experimental—chemistry

Materials

Melting points were measured by Barnstead Electrothermal IA9200 and are uncorrected. ^{1}H- and ^{13}C-NMR spectra were recorded on Varian Gemini (300/600 MHz and 75/150 MHz, resp.), chemical shifts are given in parts per million (ppm), tetramethylsilane was used as an internal standard and DMSO-*d6* as the solvent, unless otherwise specified. IR spectra were acquired on FT-IR-ATR REACT IR 1000 (ASI Applied Systems) with diamond probe and MTS detector. Mass spectra were performed on LC–MS (Agilent Technologies 1200 Series equipped with Mass spectrometer Agilent Technologies 6100 Quadrupole LC–MS). The course of the reactions was followed by TLC analysis (Merck Silica gel 60 F254). UV lamp (254 nm) and iodine vapours were used for the visualization of TLC spots. Starting chemicals were purchased from Sigma-Aldrich, Fluorochem, AlfaAesar or Acros vendors.

Synthesis of (*E*)-3-(pyridin-3-yl)-1-(pyridin-4-yl) prop-2-en-1-one (3PO)

To a solution of 884 mg (8.26 mmol, 1.00 mol eq) nicotinaldehyde **1** and 1.00 g (8.26 mmol, 1.00 mol eq) of pyridinylethanone **2** in 2 ml of glacial acetic acid, 1.12 g (13.7 mmol, 1.65 mol eq) of AcONa was added. The mixture was heated to reflux overnight. Afterwards TLC analysis confirmed only a spot for a new product. The reaction was cooled down, 10 ml of water added and the mixture has been stirred within 2 h at RT. Obtained solid material was filtered off, washed on a filter by H_2O (2 × 10 ml) and dried on the air. The crude product (1.25 g) was crystallised from 10 ml of boiled EtOH to yield 989 mg (4.71 mmol, 57%) of **3 (3PO)** after standing at RT and later on in a refrigerator overnight (Scheme 2). Obtained **3PO** (Fig. 2) forms pale yellow solid material. **M.p.:** 144.4–145.9 °C [EtOH] (lit.: 146–147 °C [H_2O]) (Durinda et al. 1966).

^{1}H-NMR (600 MHz, DMSO-*d6*): δ 9.00 (d, 1H, $J(B_2,B_4) = 1.8$ Hz, H–C_B(2)), 8.83 (d, 2H, $J(A_2,A_3) = 6.0$ Hz, 2 × H–C_A(2)), 8.61 (dd, 1H, $J(B_5,B_6) = 4.7$ Hz, $J(B_4,B_6) = 1.5$ Hz, H–C_B(6)), 8.33 (ddd, 1H, $J(B_4,B_5) = 7.9$ Hz, $J(B_2,B_4) = 1.8$ Hz, $J(B_4,B_6) = 1.5$ Hz, H–C_B(4)), 7.98 (d, 1H, J(CH = CH) = 15.8 Hz, –CH = C(2)HCO–), 7.97 (d, 2H, $J(A_2,A_3) = 6.0$ Hz, 2 × H–C_A(3)), 7.79 (d, 1H, J(CH = CH) = 15.8 Hz, –C(3)H = CHCO–), 7.51 (dd, 1H, $J(B_4,B_5) = 7.9$ Hz, $J(B_5,B_6) = 4.7$ Hz, H–C_B(5)).

^{13}C-NMR (150 MHZ, DMSO-*d6*): δ 189.4 (C = O), 151.8 C_B(6), 151.3 (2 × C_A(2)), 151.0 C_B(2), 143.7 C_A(4), 142.7 (–C(3)H = CHCO–), 135.8 C_B(4), 130.7 C_B(3), 124.5 C_B(5), 123.8 (–CH = C(2)HCO–), 122.1 (2 × C_A(3)).

FT-IR (solid, cm^{-1}): 2109 (w), 2082 (w), 1912 (w), 1671 (s), 1606 (s), 1583(s), 1552 (s), 1473 (m), 1415 (s), 1353 (m), 1303 (s), 1218 (s), 1120 (m), 1096 (m), 1021 (s), 982 (s), 878 (m), 836 (m), 793 (s).

MS (ESI m/z): 211.1 $[M+H]^+$.

Anal. Calcd for $C_{13}H_{10}N_2O$ (210.23): C, 74.27; H, 4.79; N, 13.33. Found: C, 74.02; H, 4.89; N, 13.48.

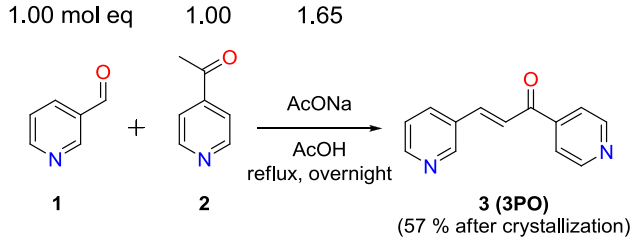

Scheme 2 The novel synthesis of **3PO** performed from **1** and **2** by AcONa in refluxing AcOH

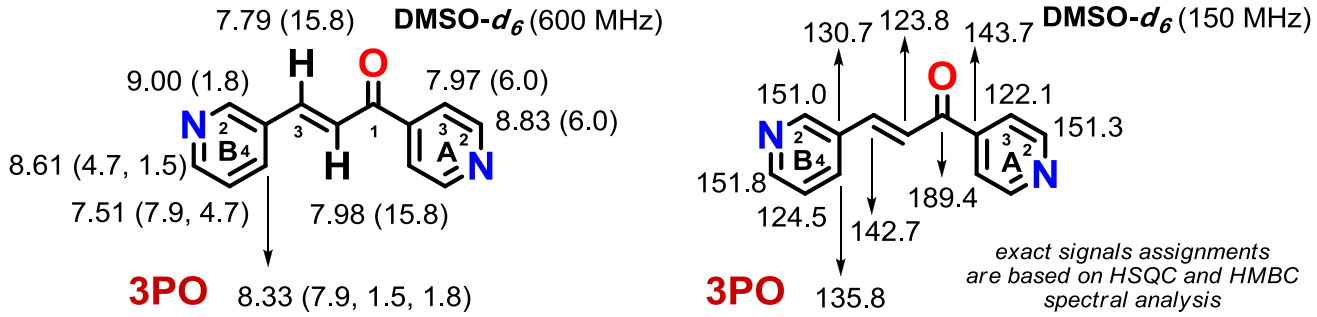

Fig. 2 ^{1}H and ^{13}C-NMR diagrams of **3PO**. Exact chemical shift assignments are based on 2D NMR spectral analysis (HSQC and HMBC)

Experimental—biology

Materials

Cell lines and reagents

Human umbilical vein endothelial cells (HUVECs) were obtained in cooperation with Eurocord Slovakia (2018). Cells were isolated from fresh umbilical cords as described in the literature (Moravčík et al. 2016). Cells were incubated in a complete endothelial cell growth medium (ECGM; Promo Cell, Germany) containing endothelial cell growth supplements (ECGS; Promo Cell, Germany). Cells were incubated in the humidified incubator (Heal Force Bio-meditech, China) at standard conditions (in 5% CO_2 at 37 °C). In the presented experiments, cells at lower passages (3–5) were used.

Glucose metabolism inhibitor **3PO** was synthesized as described in this paper. Multi-kinase inhibitor in the form of its salt **sunitinib l-malate** was obtained as a gift from US pharmaceutical company (Pfizer). Inhibitors were diluted in dimethyl sulfoxide (DMSO; Sigma-Aldrich) in an appropriate concentration as stock solutions and further diluted in ECGM to required concentrations. Inhibitors were used at concentrations at which no cytotoxic effects were observed.

HUVEC proliferation assays

To explore effects of **3PO** and **SU** (**sunitinib l-malate**) on proliferation of HUVEC cells, two experiments were performed. Cells were treated either with the inhibitor **3PO** alone or in a combination with kinase inhibitor **SU**. In the first trial, endothelial cells were treated with different concentrations of **3PO** (5, 10, 12.5 and 15 µM) (Fig. 3). In the second trial, the combined effect of **3PO** and multi-kinase inhibitor **sunitinib (SU)** on HUVEC cell proliferation was evaluated. The cells were treated with **3PO** always at one (10 µM) and **SU** at three different concentrations (0.1, 1.0 and 10 µM) (Fig. 4).

BrdU assay

Cell proliferation was determined by the BrdU assay according to manufacturer´s instructions. (Roche, France). The measurement was based on incorporated bromodeoxyuridine (BrdU) during DNA synthesis. HUVECs were seeded in a 96-well plate at a density 2×10^3 cells/well. Cells were incubated in ECGM for 24 h at 37 °C at 5% CO_2. Subsequently, the medium was removed and cells were cultured with different concentrations of inhibitors for 24 h. Afterwards 10 µl/well of BrdU labelling solution was added for 2 h, then the medium was removed and cells were fixed and denatured in 200 µl/well FixDenat. After these cells were incubated with anti-BrdU-POD working solution for 45 min at room temperature. Excess of antibody was removed by washing the wells with washing solution. Afterwards, substrate solution was added and cells were incubated until colour development. Stop solution was added to each well after 1 min and the absorbance of the sample was measured on the Microplate spectrophotometer Mulltiskan GO (Thermo

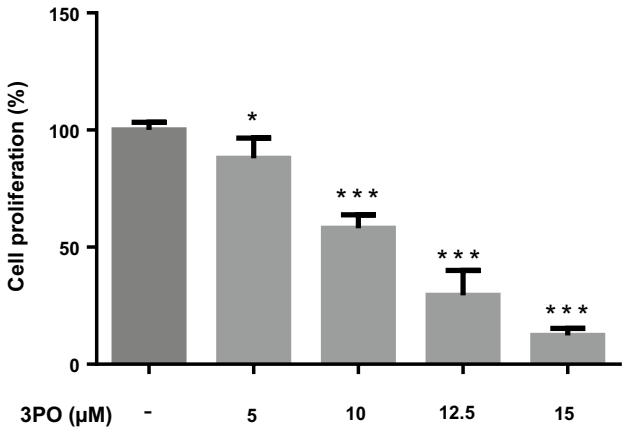

Fig. 3 Inhibitory effect of 3PO on HUVEC cell proliferation. After reaching a confluent monolayer, HUVEC cells were treated with BrdU and **3PO** at different concentrations (5–15 µM). Changes in cell proliferation were evaluated after 24 h of incubation. **3PO** allows proliferation at 5 µM (on 88%), 10 µM (59%), 12.5 µM (29%), 15 µM (12.5%) compare to untreated HUVEC control (100%). Data represent the mean ± SEM of three independent experiments. $*P<0.05$, $***P<0.001$

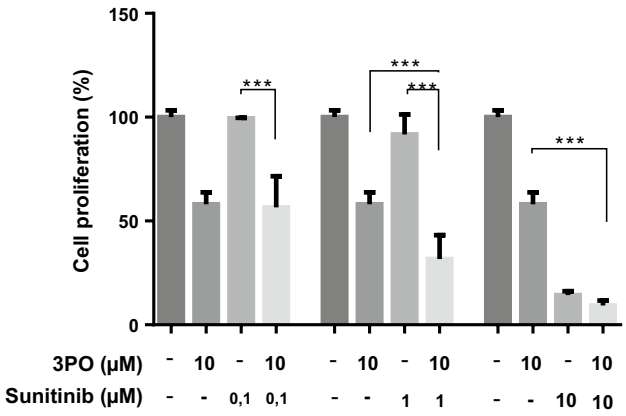

Fig. 4 Inhibitory effect of sunitinib (SU) and 3PO on a cell proliferation. After reaching a confluent monolayer, endothelial cells were treated with **3PO** at 10 µM and different doses of **SU** for 24 h. Changes in cell proliferation were evaluated after 24 h of incubation by BrdU. The high of the bars clustered in an order from the left to the right (100%, 58, 99, 57; 100%, 57, 92, 32 and 100%, 58, 14, 9). Data represent the mean ± SEM of three independent experiments. $***P<0.001$

Fisher Scientific, Waltham, USA) at 450 nm. Cell proliferation was evaluated as comparison of percentage of viable cells in treated groups to the control.

Statistics

Data were analysed statistically with ANOVA followed by the Tukey post hoc test and the differences $P < 0.05$ were considered significant.

Results and discussion

Attempts to prepare inhibitor **3PO** by different basic conditions similar as described in the literature (KOH, K_2CO_3, Et_3N) at RT (or by cooling) within shorter or longer time were not successful and only traces of **3PO** were formed. Therefore, we concluded that the basic (nucleophilic) conditions are not convenient for the synthesis of **3PO** due to its high reactivity and fast transformation within reaction conditions to the complex side products. This was in agreement with the published data (Vatsadze et al. 2004) (Scheme 1). Only the synthesis of **3PO** performed with Et_2NH at RT described by (Durinda et al. 1966 and 1967) gave required **3PO** in a low 12% yield after FLC purification. The reaction performed in the presence of Et_2N is more complex compared to the one with Et_3N and can perform partially through an enamine mechanism see Scheme S(1–2) in the Supporting material. At the end, we had to develop a novel and efficient synthesis of **3PO** by condensation of the nicotinaldehyde **1** and the pyridinylethanone **2** by AcONa in refluxing AcOH (Scheme 2). The yield of **3PO** was 57% after crystallisation from hot EtOH. Missing physico-chemical properties and spectra of **3PO** in the literature were determined also by a help of 2D-NMR techniques (HSQC, HMBC) (Fig. 2). The figures of **3PO** spectra and the HMBC analysis are in the Supporting material.

The inhibitor **3PO** alone dose-dependently decreased proliferation of HUVECs compared to control (Fig. 3).

In the second trial, the combined action of **3PO** at 10 μM and **SU** at 1 μM significantly decreased cell proliferation in comparison with cells treated with inhibitors applied individually. Combined screening of **3PO** at 10 μM with **SU** at the higher (10 μM) and the lower (0.1 μM) concentration did not meaningly decrease the cell proliferation compared to **SU** or **3PO** alone.

Glycolysis inhibitor **3PO** applied alone dose-dependently inhibited HUVEC cell proliferation in comparison to control: 5 μM (− 12%), 10 μM (− 41%), 12.5 μM (− 71%), 15 μM (− 87%) (Fig. 3). The combined effect of **3PO** (10 μM) and multi-kinase inhibitor **sunitinib l-malate (SU)** (1–10 μM) was synergistically effective only at 1 μM concentration. **SU** applied at higher or lower concentrations did not show a synergistic effect (Fig. 4, Table 1).

Table 1 The summary of a percentage of the HUVEC proliferation in the presence of **3PO** (glycolysis inhibitor) or combination **3PO** with **SU** (multi-kinase inhibitor) compare to a control (see also Figs. 3 and 4)

	Treated HUVEC proliferation[a] (%)	Combined experiments[a] **3PO** (10 μM) + **SU**
3PO (5 μM)	88	–
3PO (10 μM)	59	–
3PO (12.5 μM)	29	–
3PO (15 μM)	12.5	–
		57–58% (without **SU**)
SU (0.1 μM)	99	57%
SU (1 μM)	92	**32%**
SU (10 μM)	14	9%

[a]Based on an untreated HUVEC proliferation (100%)

Inhibitor **3PO** blocks PFKBF3 (an important enzyme of glycolysis) with relatively low enzymatic activity ($IC_{50} = 22.9$ μM) (Fig. 1). However, **3PO** inhibited HUVECs proliferation twice more effectively ($IC_{50} = 10.7$ μM, calculated from an experiment depicted on Fig. 3). This finding suggests that activity of **3PO** is more complex and not limited to only one target, e.g. PFKBF3.

Conclusions

According to procedures from the literature, the preparation of **3PO** by condensation of nicotinaldehyde **1** and pyridinylethanone **2** under basic conditions (KOH, K_2CO_3, Et_3N) at various temperatures and times was unsuccessful in our hands. The resulting **3PO** is susceptible on nucleophilic attack and rapidly undergoes further transformations within the reaction to form a mixture of polar by-products (Scheme 1) (Vatsadze 2004). Repeating the reaction in the presence of Et_2NH (Durinda et al. 1966 and 1967), we prepared **3PO** only on 12% yield after FLC purification (Scheme S1) (see Supplementary Material). This reaction performs probably because of formation of an enamine intermediate protecting the precursor of the product from degradation and required compound **3PO** occurred after an acidic reaction workup. The proposed mechanism is shown in Scheme S2 (see Supplementary Material). The low 12% yield of the above reaction indicates that Et_2NH has basic properties and the reaction could perform also towards to the undesired by-products (similar as in cases when KOH, K_2CO_3 or Et_3N were used). Therefore, we have developed novel reaction conditions for an efficient preparation of **3PO** by condensation of nicotinaldehyde **1** and pyridinylethanone

2 in the presence of AcONa in refluxing concentrated acetic acid. Thus, **3PO** can be prepared in 57% yield after purification by crystallisation from a hot EtOH (Scheme 2). The compound **3PO** was fully characterized and further used in biological experiments.

We found that glycolysis inhibitor **3PO** dose-dependently (5, 10, 12.5 and 15 μM) inhibits HUVEC cell proliferation (− 12, − 42, − 71 and − 88% compare to control). Combined screening of **3PO** (10 μM) with multi-kinase inhibitor **sunitinib l-malate** exhibited a synergistic effect at **SU** concentration 1 μM (− 68%) [alone: **3PO** 10 μM (− 42%) and **SU** 1 μM (− 8%)]. However, higher (10 μM) and also lower (0.1 μM) concentration of **SU** did not show synergy effect (Fig. 4).

The small planar unsaturated compound **3PO** (FW: 210.23) identified in the literature as an inhibitor of an important glycolytic enzyme (IC_{50} = 22.9 μM, PFKFB3, Clem et al. 2013) has been shown to be more as twice as effective in cell assay as an inhibitor of endothelial cell proliferation (IC_{50} = 10.7 μM, HUVECs). This finding indicates that **3PO** should be able to inhibit also other important biological target(s) in addition to PFKFB3. Based on a chemical structure and observed reactivity of **3PO** we can propose its ability to inhibit biological target(s) also by a non-competitive manner, e.g. after binding of –SH group of some cysteine residue from a biological target to the α,β-unsaturated enone fragment of **3PO** (the Michael addition).

Acknowledgements VEGA1/0670/18 and 1/0557/15; Biomagi, Ltd. (novel synthesis of **3PO**, proposals: mechanism of Et_2NH, multi-target **3PO** properties). This publication is partially also the result of the project implementation: Comenius University in Bratislava Science Park supported by the Research and Development Operational Programme funded by the ERDF. Grant number: ITMS 26240220086.

Compliance with ethical standards

Conflict of interest On behalf of all authors, the corresponding author states that there is no conflict of interest.

References

Carmeliet P, Jain RK (2011) Molecular mechanisms and clinical applications of angiogenesis. Nature 473:298–307. https://doi.org/10.1038/nature10144

Clem BF, O'Neal J, Tapolsky G, Clem AL, Imbert-Fernandez Y, Kerr DA 2nd, Klarer AC, Redman R, Miller DM, Trent JO, Telang S, Chesney J (2013) Targeting 6-phosphofructo-2-kinase (PFKFB3) as a therapeutic strategy against cancer. Mol Cancer Ther 12:1461–1470. https://doi.org/10.1158/1535-7163

Conradi L-C, Brajic A, Cantelmo AR, Bouché A, Kalucka J, Pircher A, Brüning U, Teuwen L-A, Vinckier S, Ghesquière B, Dewerchin M, Carmeliet P (2017) Tumor vessel disintegration by maximum tolerable PFKFB3 blockade. Angiogenesis 20:599–613. https://doi.org/10.1007/s10456-017-9573-6

De Bock K, Georgiadou M, Schoors S, Kuchnio A, Wong BW, Cantelmo AR, Quaegebeur A, Ghesquière B, Cauwenberghs S, Eelen G (2013) Role of PFKFB3-driven glycolysis in vessel sprouting. Cell 154:651–663. https://doi.org/10.1016/j.cell.2013.06.037

Durinda J, Szucs L, Krasnec L, Heger J, Springer V, Kolena J, Keleti J (1966) Chemistry and biological properties of azachalcones. Acta Facultatis Pharmaceuticae Bohemoslovenicae 12:89–129 **(Chem. Abstr. 1968 68: 114494y)**

Durinda J, Kolena J, Szücs L, Krasnec L, Heger J (1967) Study of adrenal cortex inhibitors of the amphenone group. I. Azachalcones Ceskoslovenska farmacie 16:14–15 **(PMID: 6044302)**

Eurocord-Slovakia http://eurocord.sk/. Accessed 30 May 2018

FDA (U.S. Food and Drug Administration). https://www.fda.gov. Accessed 30 May 2018

Ferrara N, Hillan KJ, Gerber H-P, Novotny W (2004) Discovery and development of bevacizumab, an anti-VEGF antibody for treating cancer. Nat Rev Drug Discovery 3:391–400. https://doi.org/10.1038/nrd1381

Jeong B-S, Choi H, Kwak Y-S, Lee E-S (2011) Synthesis of 2,4,6-Tripyridyl pyridines, and evaluation of their antitumor cytotoxicity, topoisomerase i and ii inhibitory activity, and structure-activity relationship. Bull Korean Chem Soc 32:3566–3570. https://doi.org/10.5012/bkcs.2011.32.10.3566

Kerbel R, Folkman J (2002) Clinical translation of angiogenesis inhibitors. Nat Rev Cancer 2:727–739. https://doi.org/10.1038/nrc905

Lintnerová L, García-Caballero M, Gregáň F, Melicherčík M, Quesada AR, Dobiaš J, Lác J, Sališsová M, Boháč A (2014) A development of chimeric VEGFR2 TK inhibitor based on two ligand conformers from PDB: 1Y6A complex—medicinal chemistry consequences of a TKs analysis. Eur J Med Chem 72:146–159. https://doi.org/10.1016/j.ejmech.2013.11.023

Liptaj T, Mlynarik V, Remko M, Durinda J, Heger J (1981) ^{13}C-NMR spectra of azachalcones. Collect Czech Chem Commun 46:1486–1491. https://doi.org/10.1135/cccc19811486

Moravčík R, Stebelová K, Boháč A, Zeman M (2016) Inhibition of VEGF mediated post receptor signalling pathways by recently developed tyrosine kinase inhibitor in comparison with sunitinib. Gen Physiol Biophys 35:511–514. https://doi.org/10.4149/gpb_2015055

Pisarsky L, Bill R, Fagiani E, Dimeloe S, Goosen RW, Hagmann J, Hess Ch, Christofori G (2016) Targeting metabolic symbiosis to overcome resistance to anti-angiogenic therapy. Cell Rep 15:1161–1174. https://doi.org/10.1016/j.celrep.2016.04.028

Pla AF, Brossa A, Bernardini M, Genova T, Grolez G, Villers A, Leroy X, Prevarskaya N, Gkika D, Bussolati B (2014) Differential sensitivity of prostate tumor derived endothelial cells to sorafenib and sunitinib. BMC Cancer 14:939. https://doi.org/10.1186/1471-2407-14-939

Reaxys DB (2018) https://www.reaxys.com. Accessed 30 May 2018

Schoors S, De Bock K, Cantelmo AR, Georgiadou M, Ghesquière B, Cauwenberghs S, Kuchnio A, Wong BW, Quaegebeur A, Goveia J (2014) Partial and transient reduction of glycolysis by PFKFB3 blockade reduces pathological angiogenesis. Cell Metab 19:37–48. https://doi.org/10.1016/j.cmet.2013.11.008

SciFinder DB (2018) https://scifinder.cas.org. Accessed 30 May 2018

Shaheen RM, Tseng WW, Davis DW, Liu W, Reinmuth N, Vellagas R, Wieczorek AA, Ogura Y, McConkey DJ, Drazan KE (2001) Tyrosine kinase inhibition of multiple angiogenic growth factor receptors improves survival in mice bearing colon cancer liver metastases by inhibition of endothelial cell survival mechanisms. Can Res 61:1464–1468 **PMID: 11245452**

Tejpar S, Prenen H, Mazzone M (2012) Overcoming resistance to antiangiogenic therapies. Oncologist 17:1039–1050. https://doi.org/10.1634/theoncologist.2012-0068

WSS Inc. US (2018) Spectral data were obtained from Wiley Subscription Services, Inc. (US)

Vatsadze SZ, Nuriev VN, Leshcheva IF, Zyk NV (2004) New aspects of the aldol condensation of acetylpyridines with aromatic aldehydes. Russ Chem Bull 53:911–915. https://doi.org/10.1023/b:rucb.0000037863.85554.35

Zecchin A, Kalucka J, Dubois C, Carmeliet P (2017) How Endothelial Cells Adapt Their Metabolism to Form Vessels in Tumors. Front Immunol 8:1750. https://doi.org/10.3389/fimmu.2017.01750